The Shape of Rupture Surface in Dry Sand

La forme de la surface de rupture dans le sable sec

by A. R. JUMIKIS, Dr. Eng. Sc., Professor of Soil Mechanics and Foundation Engineering, Rutgers, The State University, College of Engineering, Department of Civil Engineering, New Brunswick, New Jersey, U.S.A.

Summary

The purpose of this paper is to present the results of an experimental study about the shape of the rupture surface and on the effect of the width of a foundation model, loaded obliquely, on the shape of the rupture surface in dry sand. Five models of various widths were loaded obliquely with a constant, vertical, average contact pressure of $\sigma = 1{\cdot}00$ kg/cm^2.

The experimental study permitted the observation that the sheared-off sand wedge is expelled one-sidedly as an almost solid body along a curved rupture surface. The study brought out that the rupture surface coincides very closely with the polar curve of a logarithmic spiral. The wider the model, the larger and more deeply seated are the spirals. With narrow widths, $B = 5{\cdot}0$ cm, 7·5 cm and 10·0 cm, the spirals are almost of the same size. The larger the spiral the higher its pole. The spirals for different widths of the foundation model were found to be similar.

The results of this study suggest their possible application to bearing capacity and stability calculations of long strip foundations loaded obliquely.

Sommaire

L'objet de cet article est de présenter les résultats d'une étude expérimentale de la forme de la surface de rupture et de l'influence que la largeur d'un modèle d'une fondation obliquement chargé exerce sur la forme de la surface de rupture dans le sable sec. Cinq modèles de différentes largeurs ont été chargés obliquement avec une pression de contact verticale constante de valeur moyenne $\sigma = 1{,}00$ kg/cm^2.

L'étude expérimentale a démontré que le coin de sable est repoussé d'un côté comme une masse solide, le glissement se produisant sur une surface cylindrique. Au cours de l'étude on a constaté que cette surface de rupture se rapproche d'une surface cylindrique engendrée par une spirale logarithmique. La masse du sable déplacée atteint une profondeur d'autant plus grande que le modèle est plus large. Pour des modèles étroits, $B = 5{,}0$ cm, 7,5 cm et 10 cm, les surfaces de rupture sont presque identiques. Les pôles des spirales sont d'autant plus élevés au-dessus de la surface initiale du sol que les spirales elles-mêmes sont plus grandes. Les spirales correspondantes aux différentes largeurs du modèle sont semblables.

Les résultats de cette étude semblent applicables au calcul de la capacité portante et de la stabilité des fondations sur semelles de grandes longueurs chargées obliquement.

I. Introduction

One of the basic problems of practical importance an engineer encounters when designing rigid foundations on a soil material loaded obliquely is that of estimating the stability of such soil-foundation-load systems against their lateral translation due to a horizontal load component of the inclined resultant load, and of estimating the strength of the soil for its bearing capacity. Such estimates depend to a great extend upon the true shape of the rupture surface, or, rather, the shape, size and weight of the soil wedge being held in static equilibrium with the loaded foundation. Likewise, the position of the rupture surface relative to the foundation is of importance. By this is meant the position of the coordinates of the pole of the rupture surface relative to the foundation under various methods of loading. In particular, the mode of rupture of a soil mass brought about by an obliquely loaded foundation is relatively little understood as compared with deformations in solids.

Therefore knowledge of the shape of the rupture surface in soil caused by various modes of loading should be of scientific and technical interest to the engineering profession. The results of such a study enable one to compare theory with reality, and may help to analyze on a more rational basis the problems encountered.

II. The Study

Previous Research

Up to 1958 the author studied rupture surfaces in dry sand caused by inclined loads of various intensities which were applied to a foundation model of a constant width [1, 2, 3]. Reference [1] is relatively well documented, and contains 39 references on the subject of the shape of rupture surfaces in sand.

Present Study

Apparatus—The apparatus used in the present experimental studies is shown in Fig. 1, including five foundation models,

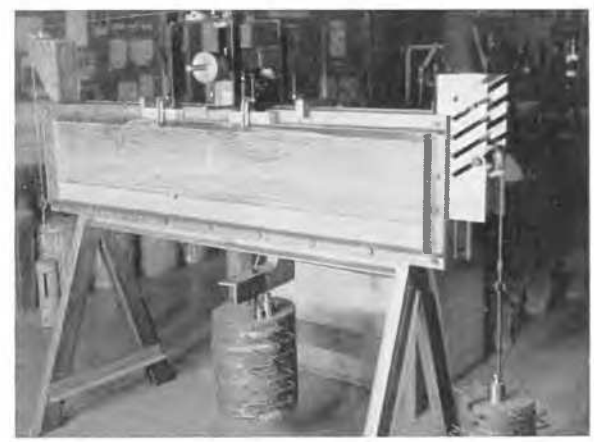

Fig. 1 Apparatus.
L'appareil.

blocks made of wood, $h = 20{\cdot}0$ cm high, $L = 15{\cdot}0$ cm deep, and $B = 5{\cdot}0$ cm, 7.5 cm, 10.0 cm, 12·5 cm and 15·0 cm wide.

Sand—Sand from the Upper Raritan Formation (Cretaceous) of the New Jersey Coastal Plain, U.S.A., was used. The particles consist of quartz, and are angular and sharp. The coefficient of internal friction was determined by the direct shear test to be $\tan \varphi = 0{\cdot}700$ ($\varphi = 35°$). The sand is very uniform ($U = 2.00 < 5$), and its particle size accumulation curve is shown in Fig. 2. The specific gravity of the sand is $Gs = 2{\cdot}65$.

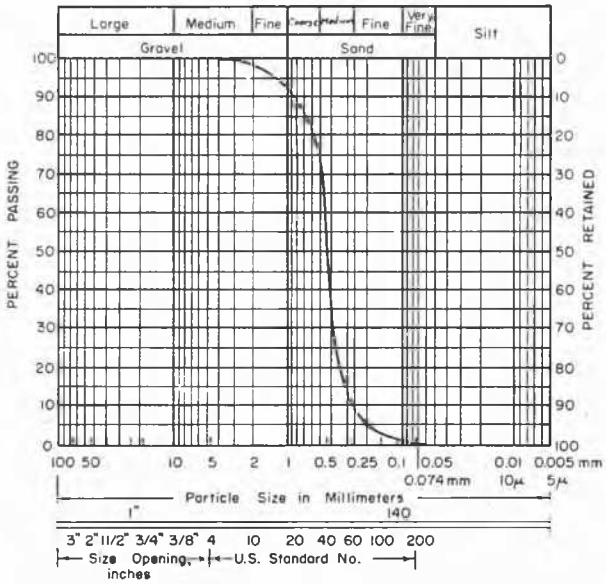

Fig. 2 Soil particle size accumulation curve.
Courbe granulométrique du sable.

The sand was placed in the experimental box with a porosity of $n \approx 43$ per cent. The relative density was a medium one : $R_D = 0{\cdot}578 \begin{matrix} < 0{\cdot}667 \\ > 0{\cdot}333 \end{matrix}$. Black-stained horizontal sand layers, approximately 3 mm thick, and spaced 10.0 mm apart, were placed in the box, along with the unstained sand, thus providing a relative medium between the unstained and stained sand. Upon failure of sand in shear, the ruptured soil wedge with the black-stained sand layers is displaced upward somewhat. The sharply sheared, black-stained layers indicate clearly the course of the rupture surface as a kind of fault lines which can be observed through the glass wall (Fig. 1).

Method of Loading—The oblique load was brought about by first applying to the foundation model from the loading yoke through a ball and socket arrangement a constant, vertical load on each of the five models of different widths. The vertical, average contact pressure on the soil under each of the five foundation models was always kept at $\sigma = 1{\cdot}00$ kg/cm^2 = const. Then a progressively increased horizontal load, H, was applied to the model at its base ($h = 0$ relative to ground surface) until the sand failed in shear.

III. The Shape of the Rupture Surface

The Force System—Statically, all the forces externally applied to the soil system, the vertical, the horizontal and the inclined forces, can be combined into one inclined resultant force, R. The free body diagram of the experimental force system is illustrated in Fig. 3.

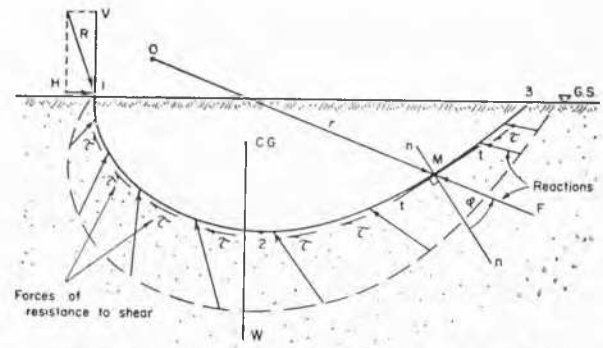

Fig. 3 Free body diagram of the experimental force system.
Diagramme des forces s'exerçant sur le système.

The rupture condition permits ascertaining the magnitude of the ultimate horizontal load, H, at which failure occurs to the system soil-model-load.

Formation of Rupture Surface—As the horizontal load, H, is gradually applied to the already vertically loaded foundation model, the latter translates gradually by sliding on the "ground" surface in the direction of the action of the horizontal load. As the horizontal load is increased the sand wedge to be ruptured begins plastic-wise and progressively vaguely to take its shape. Plastic deformation of the soil underneath the model is shown in Fig. 4.

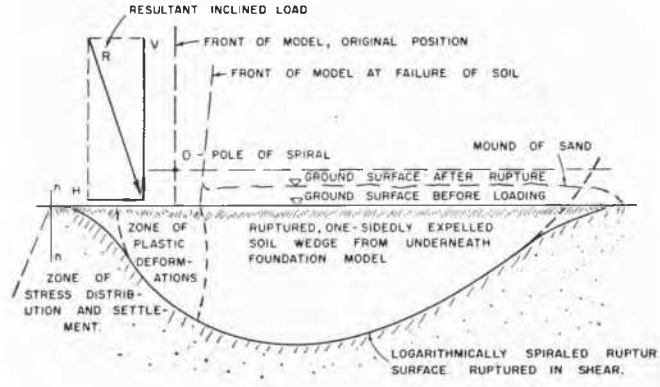

Fig. 4 Glossary of the soil-foundation-load system.
Lexique des termes employés.

Finally, upon the exhaustion of the shear strength of the sand, the sand mass ruptures without any prior warning and forms a clearly cut wedge of soil. The soil wedge slides out one-sidedly from underneath the base of the model downwards in a lateral direction and upward in a sort of rotary motion over a curvilinear cylindrical rupture or sliding surface. The rupture curve is a smooth, continuous curve, without any breaks. Measurements of the black-stained guide lines show that for most of the length of the curvilinear rupture surface the sand wedge is practically undistorted. On observing the almost undistorted and parallel black lines within the ruptured sand wedges in Figs. 5, 6, 7 and 8, for example, one gets the impression that the ruptured sand wedges behave like solid bodies.

The rupture of the sand brings about a settlement, or even the overturning of the model.

The curved rupture surfaces occur even at small loads. For example, Fig. 8 shows the shape of rupture in dry sand under a 12·5 cm wide model, the rupture being caused by an inclined load the original vertical contact pressure of which is $\sigma = 0{\cdot}25$ kg/cm^2.

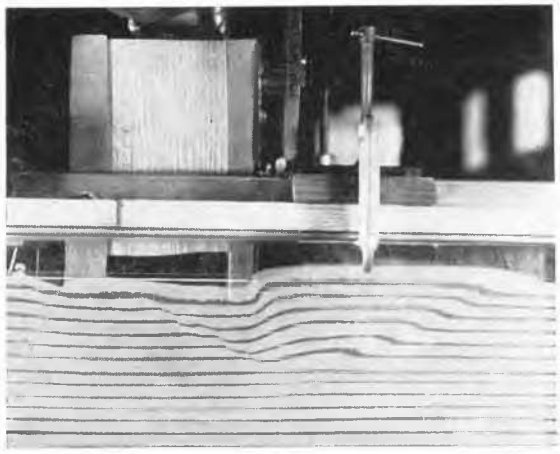

Fig. 5 Rupture surface under a $B = 15{\cdot}0$ cm wide model loaded obliquely.
Surface de rupture au-dessous d'un modèle de largeur $B = 15{,}0$ cm, chargé obliquement :
$\sigma = 1{,}00$ kg/cm² ; $h = 0$

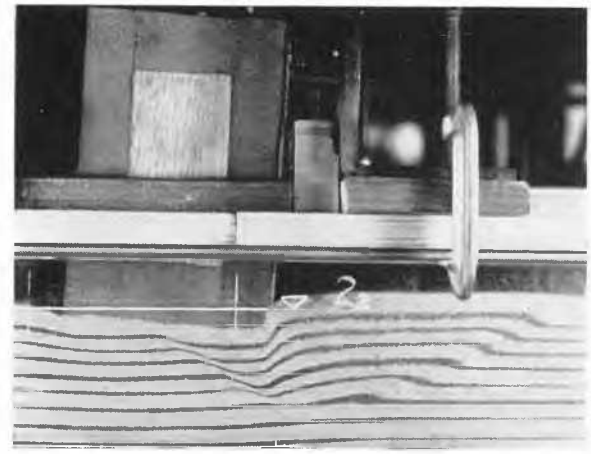

Fig. 6 Rupture surface under a $B = 12{\cdot}5$ cm wide model loaded obliquely.
Surface de rupture au-dessous d'un modèle de largeur $B = 12{,}5$ cm, chargé obliquement :
$\sigma = 1{,}00$ kg/cm² ; $h = 0$

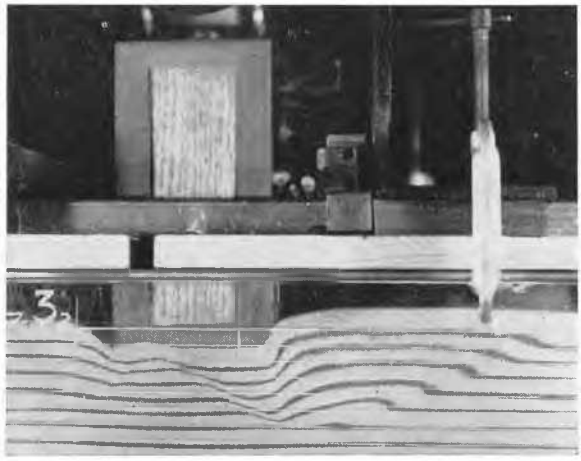

Fig. 7 Rupture surface under a $B = 1{\cdot}0$ cm wide model loaded obliquely.
Surface de rupture au-dessous d'un modèle de largeur $B = 10{,}0$ cm, chargé obliquement :
$\sigma = 1{,}00$ kg/cm² ; $h = 0$.

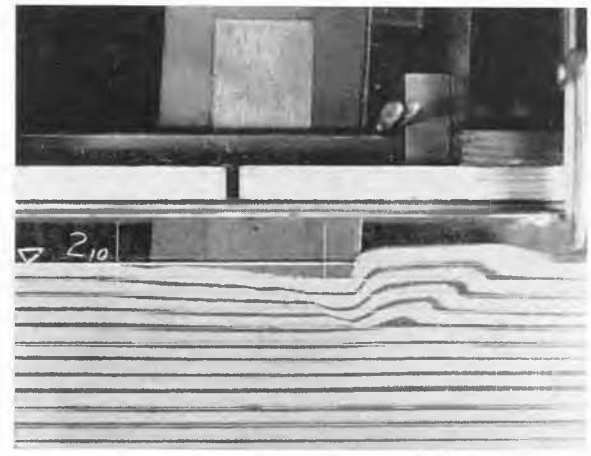

Fig. 8 Rupture surface under a $B = 12{\cdot}5$ cm wide model loaded obliquely.
La surface de rupture au-dessous d'un modèle de largeur $B = 12{,}5$ cm, chargé obliquement :
$\sigma = 0{,}25$ kg/cm² ; $h = 0$

Nature of Rupture Curve—The tracing and analysis of the rupture curves indeed bore out the concept that the shape of such curves for the particular experimental conditions agrees remarkably well with the mathematical curve of a logarithmic spiral (see Figs. 5, 6, 7 and 8).

IV. Analysis

Method.—The rupture surfaces were photographed, analyzed, grapho-analytically and mathematically studied, and an attempt was made to establish a general, physical polar equation for the observed rupture surfaces. For these experiments the physical equation of the spiral was established as a function of the inclined resultant force, R, the width of the model, B, and the angle of internal friction, φ, i.e.

$$r = f(R, B, \varphi), \text{ [mm]} \qquad (1)$$

where r = any radius-vector of the logarithmic spiral expressed in polar coordinates.

Experimental Data—The net values of the loading results of the five models are tabulated in Table 1. The H-values

Table 1
Experimental Loading Data at $\sigma = 1{\cdot}00$ kg/cm²

Model		*Loads Applied to Model*			*Ratio*
Nos.	*Width* B mm	*Vertical* V kg	*Horizontal* H kg	*Resultant* R kg	$\frac{H}{V}$
1	2	3	4	5	6
1	50	75·0	10·0 *	75·70	0·1333
2	75	112.5	22·5	114·75	0·2000
3	100	150·0	40·0	155·25	0·2666
4	125	187·5	62·5	197·60	0·3333
5	150	225.0	90·0	242.40	0·4000

* The H-values in column 4 are the best-fit values.

represent the adjusted values for the establishment of the equation $H = f(V)$. The dependence of H as a function of V, i.e. $H = f(V)$, is shown graphically in Fig. 9.

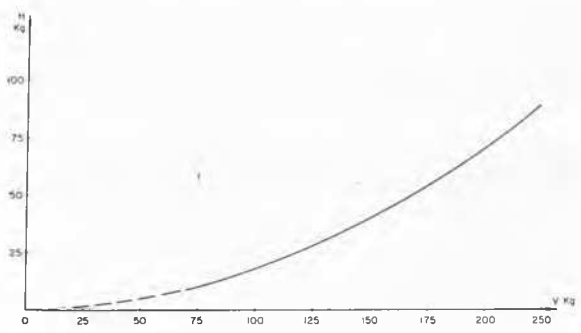

Fig. 9 Horizontal load as a function of vertical load ; $H = f(V)$.

Composante horizontale de la charge en fonction de la composante verticale ; $H = f(V)$.

The empirical equation expressing the relationship between the horizontal load, H, and the width of the model, B, was found to be

$$H = (0{\cdot}40) \cdot B^2 \left[\frac{\text{kg}}{\text{cm}^2} \right] \quad \ldots . \quad (2)$$

where B is in centimeters. Also,

$$\frac{V}{H} = (37{\cdot}5) \cdot B^{-1} \quad (3)$$

Spirals—Comparing the rupture spirals obtained from this experimental series it can be noted that they are similar for the same soil, i.e., for the same $\varphi = 35°$, their sizes differing only in the parameters. Fig. 10 shows five spirals, Nos. 1, 2, 3, 4 and 5, each corresponding to that model under which the rupture surfaces developed. The poles of the individual spirals are shown here matched in one common point 0. The horizontal lines on the left side of the spirals and below the pole, such as lines 1-1, 2-2, 3-3, 4-4 and 5-5, mean the positions of the ground surface of spirals Nos. 1 to 5 relative to the pole. This figure shows that the less the horizontal force H, the smaller and shallower is the spiral.

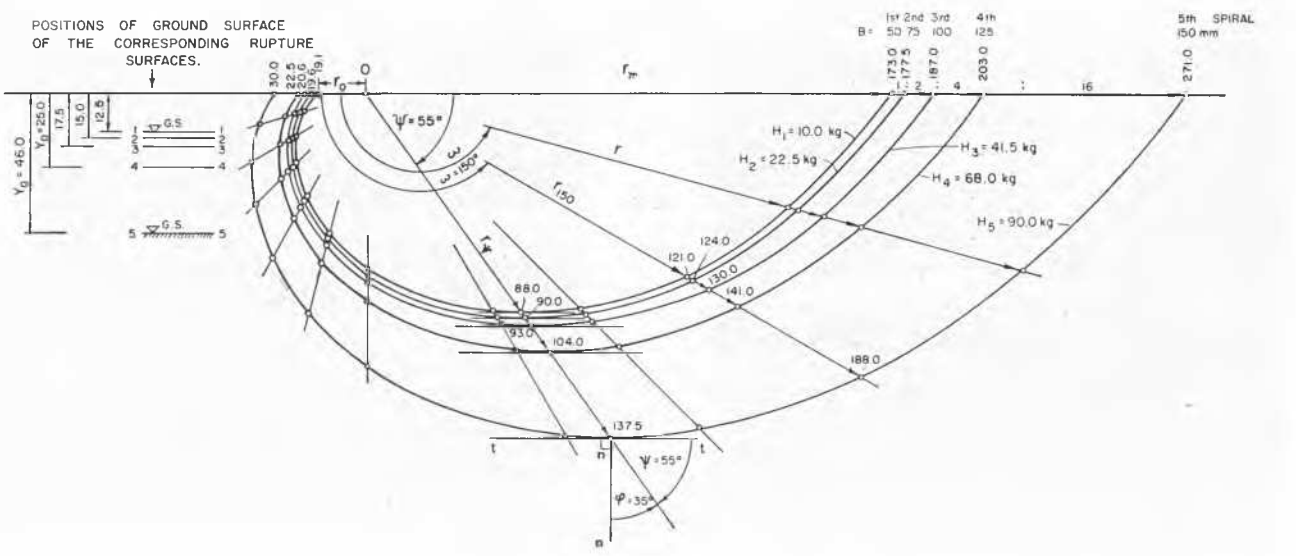

Fig. 10 Similitude of spiralled rupture surfaces (Units in millimeters).
Similitude des surfaces de rupture (dimensions en mm).

As indicated in Ref. 2, the weight, viz. the size of the spiral, is very much dependent upon the angle of internal friction, φ, of the soil in question. This is so because of the nature of the exponential function of the logarithmic spiral. This is illustrated graphically in Fig. 11.

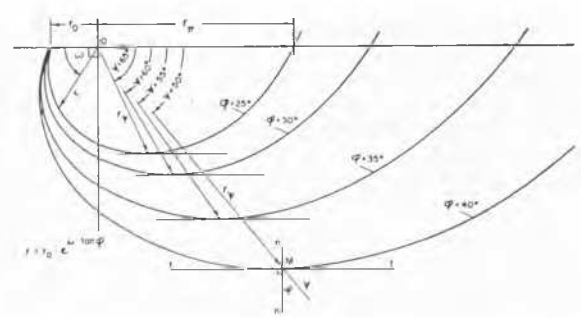

Fig. 11 Effect of angle of internal friction, φ, on shape and size of rupture surface.

Influence de l'angle de frottement interne φ sur la forme et sur les dimensions de la surface de rupture.

For purposes of comparison, Fig. 11 shows four different mathematical spirals, one for $\varphi = 25°$, one $\varphi = 30°$, one $\varphi = 35°$ and one $\varphi = 40°$, matched with their polar axes of common length, $r_o = 20{\cdot}0$ mm, and their poles in a common point 0. Note that the angle φ, viz. angle of internal friction of soil, considerably affects the shape and size if the spiral = rupture surface.

Fig. 12 shows the five experimental spirals, each of them matched against their own ground surface and against the front vertical edge of their corresponding models in their original position before the application of the horizontal loads. This Figure 12 brings out the position of the poles, 0_1, 0_2, 0_3, 0_4 and 0_5, of the five experimental spirals. Note that the smaller the spiral, the lower its pole above the ground surface. Practically the poles are located on a straight, vertical line, a line which coincides with the front vertical edge for each of the models used. On Fig. 12 the vertical coordinates, Y_0, for each pole, 0, of the spirals were measured to be

$$Y_0 = Y_1 = 12{\cdot}5 \text{ mm}$$
$$Y_2 = 15{\cdot}0 \text{ mm}$$
$$Y_3 = 17{\cdot}0 \text{ mm}$$

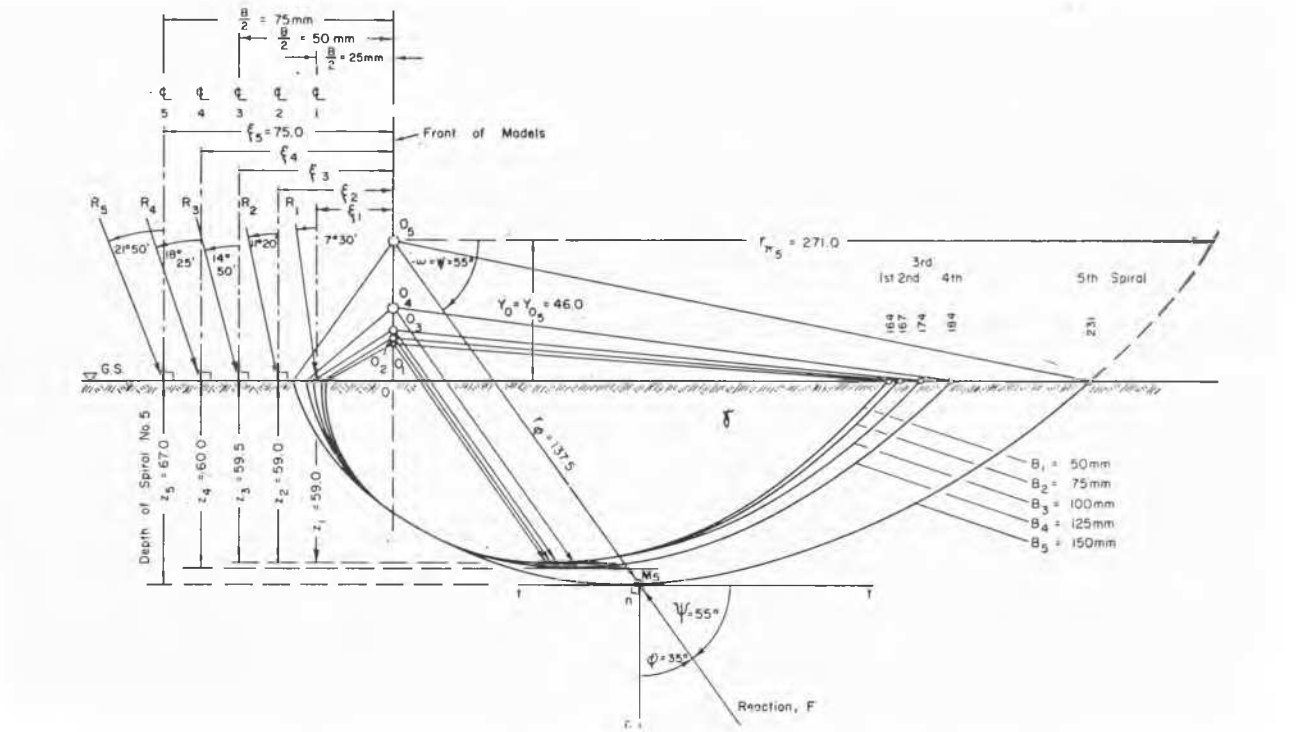

Fig. 12 Spirals matched with ground surface and front of models ; $\sigma = 1{\cdot}00$ kg/cm² ; $h = 0$.
Comparaison des spirales obtenues avec des modèles differents ; les surfaces du sol et les faces antérieures des modèles sont superposées pour illustrer la position relative des pôles ; $\sigma = 1{,}00$ kg/cm² ; $h = 0$.

$Y^4 = 25{\cdot}0$ mm
$Y^5 = 46{\cdot}0$ mm

Fig. 12 also reveals that for smaller widths of models, for instance, for $B = 50$ mm, $B = 75$ mm and $B = 100$ mm, the size of the spirals varies but little.

Some Important Radii-Vector Ratios—After establishing the poles of the spirals, it is evident from Figs. 5, 6 and 7 that the safest experimental radius-vector to measure is that having an amplitude of $\omega = 150°$, i.e. r_{150}. The empirical r_{150}-equation as a function of the resultant load, R, and width, B, of the model was determined as

$$r_{150} = B\left[(0{\cdot}263) \cdot \frac{R}{H} + 0{\cdot}374\right] \qquad (4)$$

The horizontal radius-vector, r_π, at an amplitude of $\omega = 180° = \pi$ is established as a function of r_{150} after the position of the poles was established as

$$r_\pi = (1{\cdot}44) \cdot r_{150} \qquad \ldots. \quad (5)$$

Likewise, the initial radius-vector, r_o, was established at $\omega = 0$ as follows :

All five experimental spirals have the ratio of

$$\frac{r_\pi}{r_o} = 9{\cdot}033, \qquad (6)$$

or

$$r_o = \frac{r_\pi}{9{\cdot}033}, \qquad \ldots. \quad (7)$$

or, substituting (r_π) into (r_o), from (5) into (7), obtain r_o as

$$r_o = (0{\cdot}159) \cdot r_{150} = f(R,B). \qquad \ldots. \quad (8)$$

Equation of Experimental Spirals—The equation of the experimental spirals as a function of R, B and φ has been determined as

$$r = r_o \cdot e^{\omega \cdot \tan\varphi} = B\left[(0.0406) \cdot \frac{R}{H} + 0.0578\right] \cdot e^{(0.700)\omega} \qquad \ldots. \quad (9)$$

and the position of the spirals, Y_o, may be calculated for the given systems as

$$\frac{Y_o}{r_\pi} = (0{\cdot}000016) \cdot R^{1.585} + 0{\cdot}055. \qquad \ldots. \quad (10)$$

Application of the Logarithmic Spiral to the Equilibrium Problem of a Soil Mass—Once the equation of the experimental spiral has been established, the length of the spiral, the differential sector-areas, and the areas of the segments of the spiral can be calculated in the polar coordinate system, and stability analyses of the earth masses performed.

The equilibrium condition of the soil-load system is expressed by comparing the driving and resisting moments, M_D and M_R, respectively.

Hint of Application of Spiralled Rupture Surfaces to Prototype Systems—Once the elements in the experimental models are determined as functions of R, then the load and size of the spiral of the prototype can be determined from the dynamic similitude between the model and the prototype.

The variation in size of the spirals with R and B can be made for any system similar to the model used, which had a constant length of a = 15.0 cm, by inserting the appropriate values of the physical quantities involved in the r-equation, Eq. (9).

V. Conclusions

(1) The experiments provide clear evidence of the nature of the shape of a rupture surface in dry sand caused by oblique loading of various widths, B, of foundation models loaded with a constant vertical contact pressure of $\sigma = 1{\cdot}00$ kg/cm^2.

(2) The failure of the sand mass takes place in shear. The failure depends upon the inclined load, R, the angle of internal friction, φ of the sand, the width of the model, B, and the point of application of R. Any other element of the spiral, such as r_o, r_π, Y_o and others, depends upon R and B, and also φ.

(3) The shape of the rupture surface is curvilinear and smooth throughout.

(4) The study of the experimental sliding surface corroborates that it coincides very closely with the arc of the mathematical curve of a logarithmic spiral.

(5) The experimental spirals are similar (Fig. 10).

(6) The angle of internal friction, φ, of the soil has a paramount influence on the size of the spiral, viz. bearing capacity of the soil (Fig. 11). The larger φ is, the larger the spiral.

(7) The larger R is, the larger the spiral (Fig. 12).

(8) A soil will withstand a greater horizontal load component of the inclined load, R, the wider the model.

(9) The larger the width of the model, the more deeply seated is the spiralled rupture surface (Fig. 12).

(10) The larger the spiral, the higher is the pole of the spiral above the ground surface (Y_o in Fig. 12).

(11) The results of this experimental research are useful in studying the ultimate bearing capacity of sand soil at or below the ground surface, and the nature of the rupture surface in sand formed by failure in shear. The experimental research results are also of significance in checking published theoretical information, and in analyzing the limits of its application.

Acknowledgment

These experiments were performed in the Soil Mechanics and Foundation Engineering Laboratory at Rutgers, The State University. The study was sponsored by the College of Engineering. For this the author is grateful to Dr. E.C. Easton, Dean, College of Engineering, Dr. M.L. Granstrom, Chairman of the Department of Civil Engineering, and Professor J.J. Slade, Jr., Research Director of the Bureau of Engineering Research, all of Rutgers University. Mrs. Ruth Ahrens, B.A., edited the paper. Mr. A. Shrier, M.S., was kind enough to prepare the French translation.

References

[1] A. R. Jumikis (January, 1956). Rupture Surfaces in Sand under Oblique Loads, *Proceedings of the American Society of Civil Engineers*, New York, pp.SM1-SM26.

[2] A. R. Jumikis (August, 1957). Discussion by A. R. Jumikis on 'Earth Pressures and Bearing Capacity Calculations by Generalized Procedures of Slices', by N. Janbu. *Proceedings of the Fourth International Conference on Soil Mechanics and Foundation Engineering*, London, Butterworths Scientific Publications, London, 1958, vol. III, pp. 235-238.

[3] A. R. Jumikis (Sept. 7-12, 1959). Discussion by A. R. Jumikis on 'An Investigation of Krey's Method for Bearing Capacity', by R. E. Hasson and E. Vey. *Proceedings of the First Panamerican Congress on Soil Mechanics and Foundation Engineering*, University City, Mexico, vol. II.